Physics Letters A 469 (2023) 128765

Contents lists available at ScienceDirect

Physics Letters A

journal homepage: www.elsevier.com/locate/pla

Controlling optical switching by an external magnetic field in a degenerate vee-type atomic medium

Hoang Minh Dong [a,*], Thai Doan Thanh [a], Nguyen Thi Thu Hien [a,b], Luong Thi Yen Nga [b], Nguyen Huy Bang [b,*]

[a] Ho Chi Minh City, University of Food Industry, Ho Chi Minh City, Viet Nam
[b] Vinh University, 182 Le Duan Street, Vinh City, Viet Nam

ARTICLE INFO

Article history:
Received 6 October 2022
Received in revised form 21 February 2023
Accepted 8 March 2023
Available online 14 March 2023
Communicated by B. Malomed

Keywords:
Degenerate atomic medium
Optical switching
Optical bistability
Magneto-optical switching
Electromagnetically induced transparency
Magnetic field

ABSTRACT

This paper proposes a simple model to study the optical switching behavior of low-light intensities in a degenerate V-configuration atomic system. It is shown that the optical bistability and switching properties of the system in the resonant regime can be controlled by changing the intensity of the magnetic or coupling field. The external magnetic field is used not only to realize magneto-optical switching but also to assist the system in working at varying frequency domains for the probe field without changing the frequency of the coupling field. Moreover, the switching properties also depend on the coupling field strength, detuning, and atomic cooperation parameter. The studied scheme may be helpful for applications in optical switching optimization and signal processing.

1. Introduction

Light switching light is essential in optical communication systems and quantum computers thanks to exceptional characteristics such as low switching power, high switching speed, and low signal loss [1]. As a result, many studies have been on all-optical switching based on the optical bistability (OB) mechanism in two-level systems [2]. However, traditional optical bistability systems have limitations for applications because the behavior of the bistability curves of the received signal beam at the output is only controllable by the input beam itself [3]. To tackle this problem, multi-level atomic systems applying the principles of quantum coherence and quantum interference have been an alternative solution in recent studies [4]. In the past several decades, the discovery of electromagnetically induced transparency (EIT) [5,6] has yielded atomic materials with giant nonlinearities and very tiny absorption in the resonance domain. As a result, EIT materials have created many breakthrough applications in quantum and nonlinear optics, such as slow light [7], Kerr nonlinearity [8–11], ultra-slow light propagation and soliton [12–18], OB and all-optical switching [19–21], and so on. A wide range of schemes in multi-level atomic systems was proposed to investigate the behavior of OB and optical multistability (OM) [22–30]. Its distinct advantage is its capability to create a large nonlinear medium inside an optical cavity at low light intensity compared to a two-level one. Furthermore, it is easy to manipulate the optical characteristics of the multi-level atomic systems by controlling the external coupling fields.

Besides controlling the behavior of OB in a steady state, the dynamics of all-optical switching in multi-level atomic systems have been under study. Schmidt and Ram [31] have proposed pioneering research on this topic for a three-level system under EIT conditions. Afterward, Ham and his colleagues offered several methods for generating all-optical switching based on forming dark states in three-level in 2002 [32] and four-level in 2006 [33] in ion-doped crystals. In addition, Yavuz [34] proposed a switching technique on a scale of femtoseconds under the condition of two-photon absorption of an alkali metal vapor cell. Furthermore, all-optical switching was investigated through a relative phase and spontaneously generated coherence in a three-level system [35,36] and using a technique of double-dark resonance in a four-level system [37–39]. Lately, propagation dynamics and magneto-optic switching have been launched in a four-level inverted-Y atomic medium under an external magnetic field. Unlike those studies mentioned earlier, this paper aims to control bistability behavior in a steady state and the activities of all-optical switching through the propagation dynamics of a weak probing field in both a continuous wave

* Corresponding authors.
E-mail addresses: dong.gtvtmt@gmail.com (H.M. Dong), bangnh@vinhuni.edu.vn (N.H. Bang).

https://doi.org/10.1016/j.physleta.2023.128765
0375-9601/

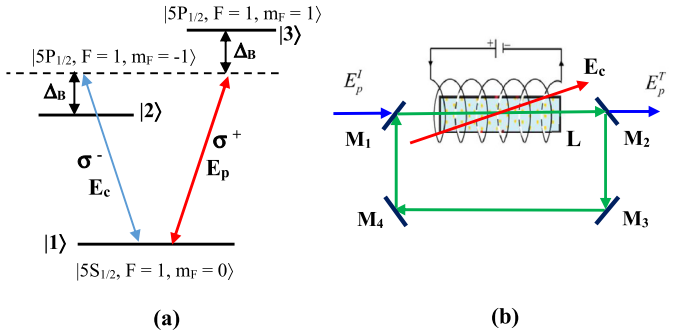

Fig. 1. (a) The degenerate vee-type atomic schema under the interaction of an external magnetic field and two laser probe and coupling fields; (b) the atomic sample has length L contained in a unidirectional ring cavity E_p^I and E_p^T is the incident and transmission fields, respectively.

mode (cw) and a pulse mode in respect of this vee-type configuration atomic system. Moreover, the model can be easily generated by experiment because of using a single laser source for both a probing beam and a coupling beam in different frequencies.

This paper investigates the coherent control of light propagation and all-optical switching in a vee-type configuration degenerate atomic medium. By simultaneously solving the Maxwell-Bloch equation systems, we indicate the independence of the absorption characteristics in the medium under the interaction of a magnetic field. Last but not least, the bistability behavior and switching dynamics of the pulse propagation process are under consideration. This proposed model may be a useful application for magneto-optic switches and magneto-optical storage devices in processing communication signals.

2. Model and basic equations

The model of the degenerate vee-type atomic system is described in Fig. 1(a). Here, the transition $|3\rangle \leftrightarrow |1\rangle$ is coupled by the σ^+ polarized probe field E_p whose Rabi frequency $\Omega_p = \mu_{31}E_p/2\hbar$. At the same time, the transition $|2\rangle \leftrightarrow |1\rangle$ is coupled with the σ^- polarized strong controlling field E_c whose Rabi frequency $\Omega_c = \mu_{23}E_c/2\hbar$. Besides, the degeneracy of the sublevels $|2\rangle$ ($m_F = -1$) and $|3\rangle$ ($m_F = +1$) is eliminated by using a longitudinal magnetic field B, which the Zeeman shift of the levels is outfitted by $\Delta_B = \mu_B m_F g_F B/\hbar$, where μ_B and g_F are the Bohr magneton and the Landé coefficients corresponding, and $m_F = \pm 1$ is the magnetic quantum number of the respective states. The decay rates from the states $|3\rangle$ and $|2\rangle$ to $|1\rangle$ are respectively given by γ_{31} and γ_{21}. Following the electric dipole approximation and the rotating wave approximations, the total Hamiltonian of the system can be given by ($\hbar = 1$) [11,40]:

$$H_{\text{int}} = \begin{bmatrix} 0 & -\Omega_c^* & -\Omega_p^* \\ -\Omega_c & -\Delta_c - \Delta_B & 0 \\ -\Omega_p & 0 & -\Delta_p + \Delta_B \end{bmatrix}, \tag{1}$$

where $\Delta_p = \omega_{31} - \omega_p$, and $\Delta_c = \omega_{21} - \omega_c$ are the frequency detuning of the probe and control fields. The Liouville equation describes the dynamic evolution of the system [4]:

$$\frac{\partial \rho}{\partial t} = -i[H_{\text{int}}, \rho] + \Lambda\rho, \tag{2}$$

Using equations (1) and (2), the density matrix equations can be given by [4,11]:

$$\dot{\rho}_{11} = \gamma_{21}\rho_{22} + \gamma_{31}\rho_{33} - i\Omega_c\rho_{12} + i\Omega_c^*\rho_{21} - i\Omega_p\rho_{13} + i\Omega_p^*\rho_{31}, \tag{3a}$$

$$\dot{\rho}_{22} = -\gamma_{21}\rho_{22} - i\Omega_c^*\rho_{21} + i\Omega_c\rho_{12}, \tag{3b}$$

$$\dot{\rho}_{33} = -\gamma_{31}\rho_{33} - i\Omega_p^*\rho_{31} + i\Omega_p\rho_{13}, \tag{3c}$$

$$\dot{\rho}_{21} = -\big(i(\Delta_c + \Delta_B) + \gamma_{21}/2\big)\rho_{21} - i\Omega_c(\rho_{22} - \rho_{11}) - i\Omega_p^*\rho_{23}, \tag{3d}$$

$$\dot{\rho}_{31} = \big(i(\Delta_p - \Delta_B) + \gamma_{31}/2\big)\rho_{31} - i\Omega_p(\rho_{33} - \rho_{11}) - i\Omega_c\rho_{32}, \tag{3e}$$

$$\dot{\rho}_{32} = i(\Delta_p - \Delta_c - 2\Delta_B)\rho_{32} + i\Omega_p^*\rho_{12} - i\Omega_c\rho_{31}, \tag{3f}$$

where the matrix elements $\rho_{ij} = \rho_{ij}^*$ (with $i \neq j$), and normalized condition $\rho_{11} + \rho_{22} + \rho_{33} = 1$, respectively.

Now, place the sample containing N atoms into the unidirectional ring cavity as represented in Fig. 1(b). Mirrors M_3 and M_4 are assumed to be perfectly reflectivity, while mirrors M_1 and M_2 have the reflection and transmission coefficients R and T ($T = 1 - R$). Furthermore, only the probe field E_p is propagated through the cavity and the coupling field E_c is not. The total electromagnetic field is represented by:

$$E = E_p e^{-i\omega_p t} + E_c e^{-i\omega_c t} + c.c. \tag{4}$$

Under the slowly varying envelope approximation, the probe field propagation is given by:

$$\frac{\partial E_p}{\partial t} + c\frac{\partial E_p}{\partial z} = i\frac{\omega_p}{2\varepsilon_0}P(\omega_p), \tag{5}$$

where $P(\omega_p)$ is polarization induced in transition $|1\rangle \leftrightarrow |3\rangle$:

$$P(\omega_p) = N\mu_{31}\rho_{31}. \tag{6}$$

With the constants of the perfectly tuned cavity and the steady-state limit, the boundary conditions between the input field E_p^I and the transmitted field E_p^T are described as [22]:

$$E_p(L) = E_p^T/\sqrt{T}, \qquad E_p(0) = \sqrt{T}E_p^I + RE_p(L). \tag{7}$$

The bistability behavior is caused by the reflection mechanism of mirror M_2, so if $R = 0$, there is no bistability. Using the boundary conditions and equation (7), we can obtain the input-output relationship in the mean-field limit.

$$y = x - iC\rho_{31}, \tag{8}$$

where $y = \mu_{31}E_p^I/\hbar\sqrt{T}$ and $x = \mu_{31}E_p^T/\hbar\sqrt{T}$ are the normalization of the fields, and $C = \frac{\omega_p NL|\mu_{31}|^2}{2\varepsilon_0\hbar cT}$ is the cooperation parameter. In the following section, the optical bistability behavior and optical switching are considered in more detail. The ^{87}Rb atom is applied in this model where the states $|3\rangle$, $|2\rangle$, and $|1\rangle$ are correspondingly $5P_{1/2}$ ($F = 1$, $m_F = \pm 1$), and $5S_{1/2}$ ($F = 1$, $m_F = 0$). The selected parameters are [11,40,41]: $\gamma_{21} = \gamma_{31} = 2\pi \times 5.3$ MHz,

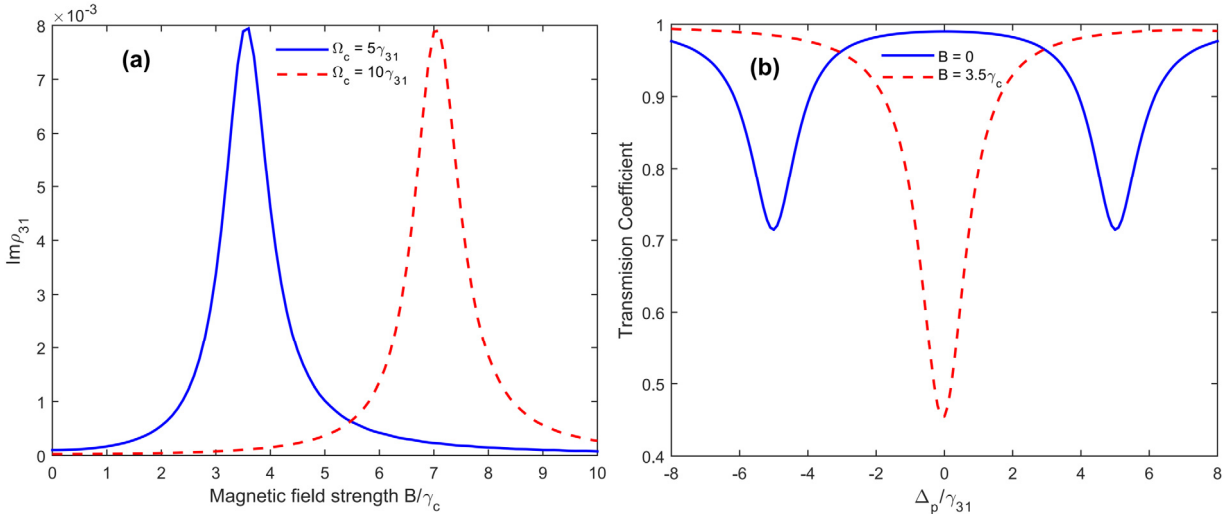

Fig. 2. (a) The probe absorption $\mathrm{Im}(\rho_{31})$ responses versus the strength of the magnetic field B at two different values of the coupling field: $\Omega_c = 5\gamma_{31}$ (solid line) and $\Omega_c = 10\gamma_{31}$ (dashed line). (b) Transmission coefficient versus the probe detuning Δ_p in the absence ($B = 0$, corresponds to the solid line) and in the presence ($B = 3.5\gamma_c$, corresponds to the dashed line) for the coupling field $\Omega_c = 5\gamma_{31}$. Other parameters are selected $\Omega_p = 0.01\gamma_{31}$, $\Delta_p = \Delta_c = 0$, and $\gamma_{21} = \gamma_{31}$, respectively.

$N = 4.5 \times 10^{17}$ atoms/m^3, $\mu_{31} = 1.6 \times 10^{-29}$ C.m., $g_F = -1/2$ and $\mu_B = 9.27401 \times 10^{-24}$ JT^{-1}. Thus, when the Zeeman shift Δ_B is expressed with respect to γ_{31}, then the magnetic field strength according to the relationship $B = \Delta_B \hbar/\mu_B m_F g_F$ should be in units of the combined constant $\gamma_c = \hbar\mu_B^{-1} g_F^{-1}\gamma_{31}$, which also has the units of the Tesla. To illustrate, when the Zeeman shift is selected as $\Delta_B = 3.5\gamma_{31}$, then the magnetic field strength $B = 3.5\gamma_c \simeq 2.65 \times 10^{-3}$ T $= 26.5$ G, respectively.

3. Numerical results and discussions

First of all, we analyze the influence of magnetic field strength B on the behavior of the probe absorption and transmission spectra. The probe absorption coefficient $\mathrm{Im}(\rho_{31})$ is the function of the magnetic field B with two different values of the coupling field intensity: $\Omega_c = 5\gamma_{31}$ (solid line) and $10\gamma_{31}$ (dashed line) as constructed in Fig. 2(a). From Fig. 2(a), it can be observed that the magnitude of the probe absorption is first on the rapid increase from nearly zero to a maximal value, then is on a dramatic decrease, and finally has the tendency to reach a small steady-state value with an increment of the magnetic field strength. Furthermore, it is noticed that the most outstanding absorption in corresponding cases of $B = 3.5\gamma_c$ for $\Omega_c = 5\gamma_{31}$ and $B = 7\gamma_c$ for $\Omega_c = 10\gamma_{31}$ at the center line of absorption spectra, while absorption is minimal in the absence of the magnetic field ($B = 0$) for all cases. Physics for the shifts from transparency to absorption of the system at the center line in the magnetic field is due to the dressed states created under the interaction of the coupling field [40]. Moreover, the higher intensity of the coupling field broadens the EIT window. The transmission coefficient for the probe field versus detuning Δ_p without and with the magnetic field is also shown in Fig. 2(b). At the line center ($\Delta_p = 0$) of the probe transmission spectrum, a complete transmission occurs and simultaneously appears two sideband deeps when the external magnetic field is turned off, whereas very low transmission arises at the center of the transmission profile when the magnetic field is turned on. Consequently, the conclusion can be drawn that the ultra-sensitive transformation from transparency to high absorption in an atomic medium exhibits a means of appropriately adjusting the intensity of the external magnetic field at a fixed intensity of the coupling field.

Next, the influence of the external magnetic field B on the shape of the OB curves is investigated by the numerical solving

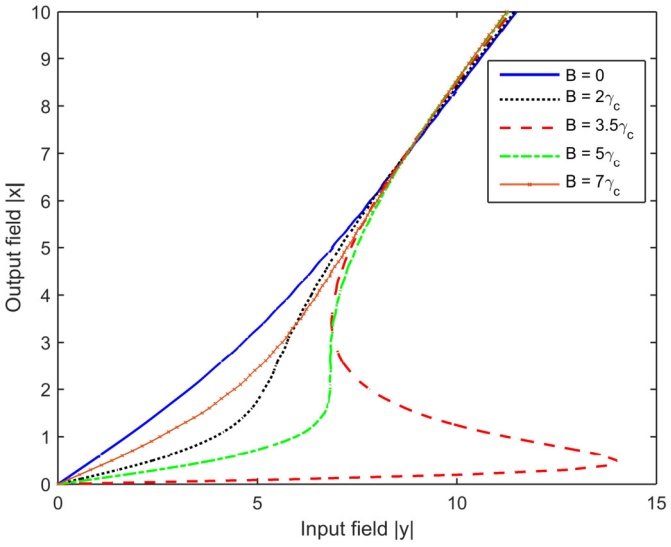

Fig. 3. Graphs of the input-output field intensity for different values of the magnetic field strength B. Other fixed system parameters are selected $\Omega_c = 5\gamma_{31}$, $\Delta_p = \Delta_c = 0$, $\gamma_{21} = \gamma_{31}$, and $C = 150$.

of equation (8) combined with equations (3) in the steady-state, as displayed in Fig. 3 and Fig. 4. Fig. 3 demonstrates some numerical results of the output field amplitude |x| against the input field amplitude |y| with different values of the intensity of the magnetic field B with other fixed parameters. By gradually increasing the intensity of the magnetic field B from 0 to $2\gamma_c$, it is obvious that the bistability appears, the hysteresis cycle commences to rise and there is a substantial increase in the threshold value. When B continues to increase up to $3.5\gamma_c$, it is found that the OB is obviously recognized, and the area of the hysteresis cycle reaches maximum. In contrast, when B increases from $3.5\gamma_c$ to $7\gamma_c$, the hysteresis cycles undergo an adverse transformation, and the bistable threshold significantly declines. Fig. 2 provides a physical mechanism for the above phenomena. When the magnetic field B ceases to exist (B=0), the levels $|2\rangle$ and $|3\rangle$ overlap each other, the absorption of the degenerate two-level medium under the EIT effect is maximally suppressed, leading to the disappearance of OB [27,28]. When the external magnetic field is put into the system, under the Zeeman effect splitting the level $|2\rangle$ and $|3\rangle$, change in the quan-

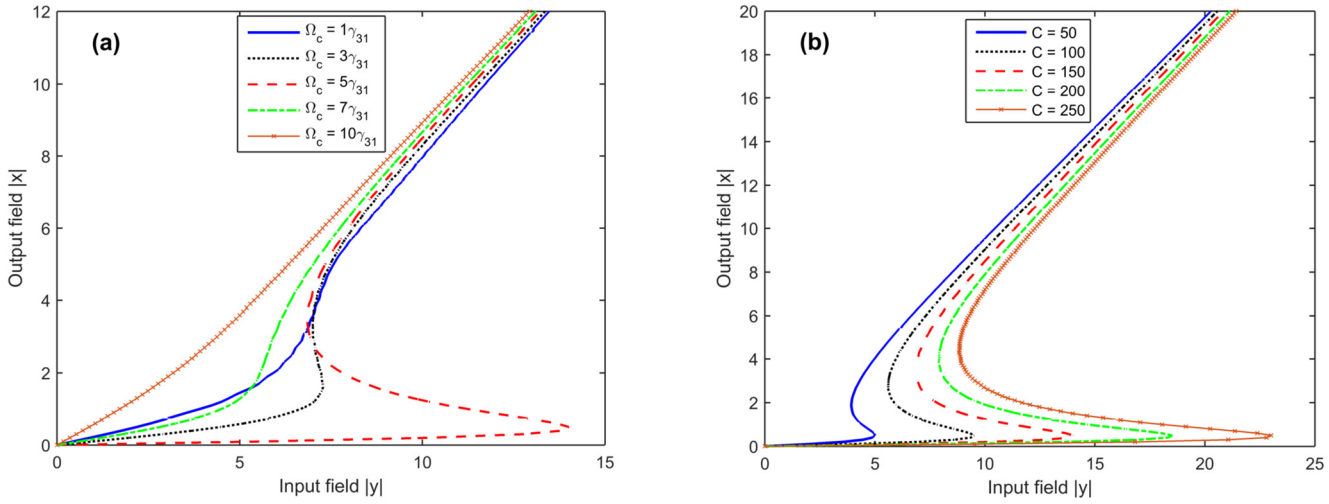

Fig. 4. (a) Graphs of the input-output field intensity with different intensities of the coupling field Ω_c with C = 150. (b) Curve diagram of the input-output field intensity with different values of the cooperation parameter C with $\Omega_c = 5\gamma_{31}$. Other parameters are kept unchanged as in Fig. 3, except $B = 3.5\gamma_c$.

tum paths between level $|1\rangle$ and level $|2\rangle$ and between level $|1\rangle$ and level $|3\rangle$ results in the decreased quantum interference, causing the increase of the absorption of the probing field. When the external magnetic field increases up to $B = 3.5\gamma_c$, both the absorption of the probing field and the optical bistability threshold reach the maximum. When B increases more, the magnitude of the absorption of the probing field significantly decreases and eventually tends to reach a steady-state value, leading to the decline of the optical bistability threshold. Such, the behavior of OB can be controlled effectively via the external magnetic field.

Fig. 4 displays the dependence of OB on the intensity of the coupling field Ω_c in Fig. 4(a) and on the atomic cooperation parameter C in Fig. 4(b), respectively. It can be seen from Fig. 4(a) that the bistable threshold is on the marked rise when the coupling field's intensity increases, then decrease gradually. In fact, by increasing the coupling field Ω_c from $1\gamma_{31}$ to a value in the neighborhood of $\Omega_c = 5\gamma_{31}$, the optical bistability threshold reaches to the maximum (red dashed line in Fig. 4(a)) because the absorption of the probe field reaches a saturated value. Nevertheless, the optical bistability threshold then decreases with an increasing the controlling field Ω_c. Physically, as the strength of the coupling field increases, the probe absorption in the transition between states $|3\rangle$ and $|1\rangle$ dramatically reduces and the nonlinearity of the medium is enhanced [11], which leads to a change in the behavior of the optical bistability. As a result, the threshold value can be easily controlled by adjusting the intensity of the coherent coupling field Ω_c. In Fig. 4(b), OB relies on the cooperation parameter C. This is called cooperation parameter C, which is proportional to the density N of the atom sample. So, an increase of parameter C leads to an enhancement of the probe absorption and increases the threshold of optical bistability.

For more practical interest and to demonstrate the analysis given in the previous parts, the propagation of a weak probe pulse through the degenerate vee-type atomic medium is addressed. From equations (5) and (6), the probe field propagation equation with Rabi frequency is obtained [14]:

$$\left(\frac{\partial}{\partial z} + \frac{1}{c}\frac{\partial}{\partial t}\right)\Omega_p(z,t) = i\alpha\rho_{31}(z,t), \tag{9}$$

where, $\alpha = \frac{\omega_p N|\mu_{31}|^2}{4\varepsilon_0 c\hbar}$ is the propagation constant, and ε_0 is the vacuum permittivity. We represent the Rabi frequency of the probe field by $\Omega_p(z,t) = \Omega_{p0} f(z,t)$, where Ω_{p0} is a real constant indicating the maximal value of the Rabi frequency at the entrance (*i.e.*, at $z = 0$), and $f(z,t)$ is a dimensionless spatiotemporal pulse-shaped function. It is convenient to transform equations (3) and (9) in a moving frame by replacing the space and time variables in the laboratory frame, z and t by those in the moving frame, ξ and τ through the relations of $\xi = z$ and $\tau = t - z/c$, with c is the speed of light. In this frame, equations (3) remains unchanged when substituting $t \to \tau$ and $z \to \xi$, while Eq. (9) can be rewritten as [14,21]:

$$\frac{\partial f(\xi,\tau)}{\partial(\xi)} = \frac{i\alpha}{\Omega_{p0}}\rho_{31}(\xi,\tau). \tag{10}$$

In the following, we numerically solve the set of Eqs. (3) and (10) on a space-time grid by using a combination of the four-order Runge-Kutta and finite difference methods, which developed a computer code for this problem is expanded from the of our previous works [14,38]. In the slowly varying envelope at the entrance to the medium $f_m(\xi = 0, \tau)$, assume that the Gaussian function is [12,21]:

$$f(\xi = 0, \tau) = exp\left[-(ln2)(\tau - 30)^2/\tau_0^2\right], \tag{11}$$

where τ_0 is the pulse temporal width of a probe pulse at the entrance of the medium.

Fig. 5 shows the temporal evolution of the normalized probe pulse envelope $|f(\xi,\tau)|^2$ at the exit of the medium with the propagation distance $\xi = 100/\alpha$ with respect to the magnetic field B at a fixed value of the coupling field $\Omega_c = 10\gamma_{31}$. Fig. 5(a) shows the intensity spectrum of the normalized probe pulse envelope $|f(\xi,\tau)|^2$ as a function of the time τ and magnetic field strength B, whereas Fig. 5(b) demonstrates the normalized probe pulse envelope $|f(\xi,\tau)|^2$ as a function of the time τ at different values of the magnetic field B. Fig. 5 shown that the different values of the magnetic field B have a significant influence on the pulse intensity spectrum of the probing field during pulse propagation in the medium. In particular, when the magnetic field is turned off ($B = 0$), the absorption of the probing field is mostly eliminated and the atomic medium is nearly transparent with the probe pulse after a characteristic propagation distance. In other words, the probe pulse propagates through the atomic medium without degeneracy (blue solid line). Conversely, when the magnetic field is turned on ($B \neq 0$), in an increment of the intensity of the magnetic field, the intensity of the probing field was on the significant decrease. When the intensity of the magnetic field increases up to approximate value $B = 7\gamma_c$ (green dash-dotted line), the pulse of

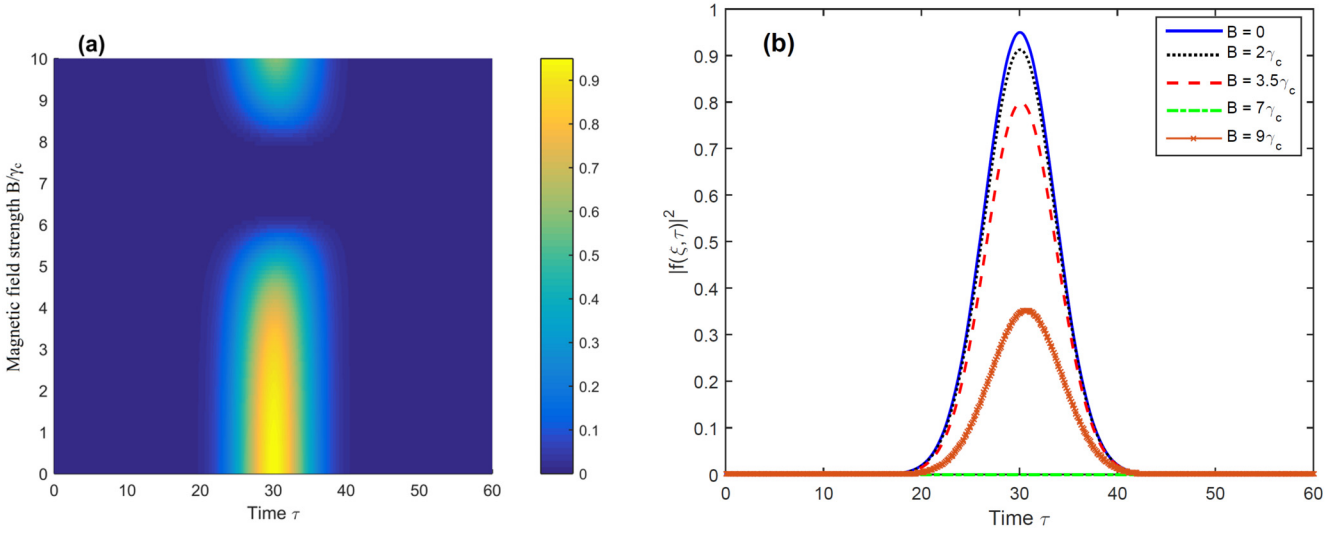

Fig. 5. (a) Intensity spectrum of the normalized probe pulse envelope $|f(\xi,\tau)|^2$ with respect to time τ and magnetic field intensity B; (b) Magnitude squared of the normalized probe pulse envelope $|f(\xi,\tau)|^2$ as a function of the time τ at the different values of the magnetic field B. Other system parameters are fixed $\Omega_{p0}=0.01\gamma_{31}$, $\Omega_c=10\gamma_{31}$, $\Delta_p=\Delta_c=0$, $\gamma_{21}=\gamma_{31}$, $\tau_0=6/\gamma_{31}$, $\xi=100/\alpha$, where time τ and propagation distance ξ are calculated in units of γ_{31}^{-1} and α^{-1}, respectively.

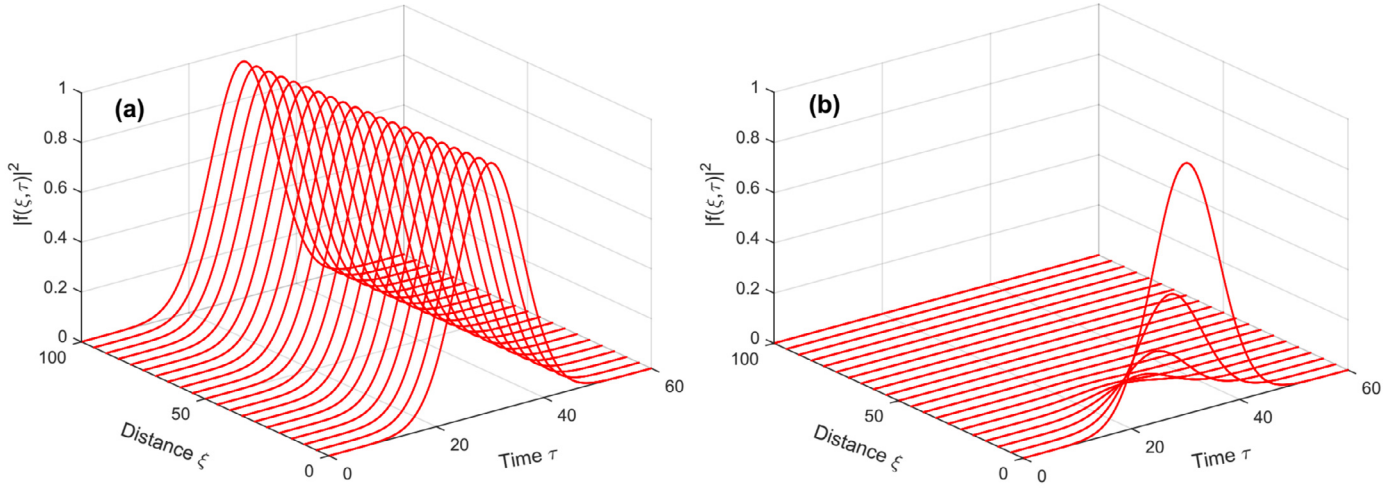

Fig. 6. Spatio-temporal evolution of the probe pulse intensity at different values of the magnetic field: $B=0$ for (a), and $B=7\gamma_c$ for (b). Other parameters are $\Omega_{p0}=0.01\gamma_{31}$, $\Omega_c=10\gamma_{31}$, $\Delta_p=\Delta_c=0$, and $\gamma_{21}=\gamma_{31}$, respectively.

the probing field is wholly absorbed by the medium in a characteristic propagation distance, so the medium eliminates the incoming probe beam. However, when the intensity of the magnetic field becomes larger $B>7\gamma_c$, the magnitude of the probe pulse increases along with the magnetic field (orange line). As a result, by selecting a suitable magnetic field value, magneto-optical modulation can be realized for such a probe pulsed signal.

Next, we illustrate the spatio-temporal evolution of the magnitude squared of the normalized probe envelopes $|f(\xi,\tau)|^2$ when the magnetic field is OFF (a) and ON (b) as shown in Fig. 6. The selected parameters are: $\Omega_{p0}=0.01\gamma_{31}$, $\Omega_c=10\gamma_{31}$, $\Delta_p=\Delta_c=0$. Fig. 6(a) shows that when the magnetic field is OFF, the medium is transparent to the probe field, so the probe pulse propagates via the medium almost without attenuation, which means that the EIT effect occurs. The probe pulse can maintain its shape at a relatively long propagation distance. Conversely, when the magnetic field is ON (and hence no EIT for the probe field), the medium becomes opaque for the probe field, and thus the probe pulse is attenuated extremely fast as entering the medium, as shown in Fig. 6(b). This mechanism is key for magneto-optical switching through the magnetic field modulation and will be illustrated in Fig. 7.

Last but not least, magnetic-optical switching for the probe field can be identified by adjusting the parameters of the magnetic field, as shown in Fig. 7. The temporal evolution of the probe field (solid line) is supposed to be a continuous wave, while the switching magnetic field is supposed to be a nearly-square pulse with increasing and decreasing smooth edges (dashed curve), and is the function of τ [21]:

$$B(\tau)=B_0\{1-0.5\tanh[0.4(\tau-10)]+0.5\tanh[0.4(\tau-35)] -0.5\tanh[0.4(\tau-60)]+0.5\tanh[0.4(\tau-85)]\}, \quad (12)$$

which is normalized by its peak value B_0, with an approximate period of $50/\gamma_{31}$. As exhibited in Fig. 7, the transmission process of the probing field is turned ON or OFF when the intensity of the magnetic field is turned OFF or ON, respectively. Consequently, with the OFF or ON switch of the magnetic field, the probe pulse can be switched anti-synchronously from ON to OFF, and vice versa. Nonetheless, the occurrence of small oscillations at the top of the front edge of the probe pulse can be observed. It can be explained that the conversion of the medium from absorption to transparency corresponds to ON and OFF mode of the magnetic

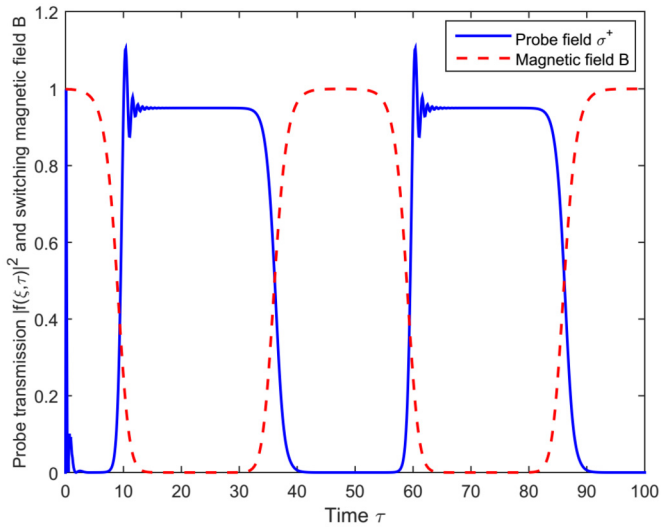

Fig. 7. Time evolution of a cw probe field (*solid line*) at $\xi = 100/\alpha$ when the magnetic field (*dashed lines*) switched at period $50/\gamma_{31}$. Other system parameters are kept constant $f(\xi = 0, \tau) = 1$, $\Omega_{p0} = 0.01\gamma_{31}$, $\Omega_c = 10\gamma_{31}$, $B_0 = 7\gamma_c$, and $\Delta_p = \Delta_c = 0$, respectively.

field, which requires a time delay. This transition delay is the reason for oscillation peaks in the front edges of the corresponding probe pulse.

4. Conclusions

In summary, through an external magnetic field modulation, we investigate magneto-optical switching and the propagation of the probing laser beam in a degenerate vee-type atomic medium. The results showed that the OB threshold could be altered by adjusting the magnetic field, the intensity of the coupling field, or the atomic cooperation parameter. Under the EIT condition, without the magnetic field, a probing laser pulse is observed to remain its shape in the medium. In contrast, when the magnetic field is present, the medium can be switched from transparency to absorption by the magnetic field being switched from OFF to ON. A near-square pulse from a continuous wave of the probe field was formed with a similar modulation period of magnetic field intensity. Consequently, the proposed model helps realize magneto-optical or optical storage switches for applications in optical communications.

CRediT authorship contribution statement

Hoang Minh Dong: Writing – review & editing, Writing – original draft, Supervision, Software, Methodology, Investigation, Formal analysis, Data curation. **Thai Doan Thanh:** Software, Formal analysis. **Nguyen Thi Thu Hien:** Investigation, Formal analysis, Data curation. **Luong Thi Yen Nga:** Methodology, Writing – review & editing. **Nguyen Huy Bang:** Writing – review & editing, Writing – original draft, Supervision, Investigation.

Declaration of competing interest

The authors declare that they have no known competing financial interests or personal relationships that could have appeared to influence the work reported in this paper

Data availability

No data was used for the research described in the article.

Acknowledgement

This research was funded by the Postdoctoral Scholarship Programme of Vingroup Innovation Foundation (VINIF), code VINIF. 2022.STS.52.

References

[1] Baojun Li, Soo Jin Chua, Optical Switches: Materials and Design, Woodhead Publishing, Limited, 2010.
[2] H.M. Gibbs, S.L. McCall, T.N.C. Venkatesan, Differential gain and bistability using a sodium-filled Fabry-Perot interferometer, Phys. Rev. Lett. 36 (1976) 1135.
[3] A.T. Rosenberger, L.A. Orozco, H.J. Kimble, Observation of absorptive bistability with two-level atoms in a ring cavity, Phys. Rev. A 28 (1983) 2569.
[4] M. Fleischhauer, A. Imamoglu, J.P. Marangos, Electromagnetically induced transparency: optics in coherent media, Rev. Mod. Phys. 77 (2005) 633.
[5] A. Imamoğlu, S.E. Harris, Lasers without inversion: interference of dressed lifetime broadened states, Opt. Lett. 14 (1989) 1344–1346.
[6] K.J. Boller, A. Imamoglu, S.E. Harris, Observation of electromagnetically induced transparency, Phys. Rev. Lett. 66 (1991) 2593.
[7] L.V. Hau, S.E. Harris, Z. Dutton, C.H. Bejroozi, Light speed reduction to 17 meters per second in an ultracold atomic gas, Nature 397 (1999) 594–598.
[8] H. Schmidt, A. Imamoglu, Giant Kerr nonlinearities obtained by electromagnetically induced transparency, Opt. Lett. 21 (1996) 1936.
[9] H.R. Hamedi, A.H. Gharamaleki, M. Sahrai, Colossal Kerr nonlinearity based on electromagnetically induced transparency in a five-level double-ladder atomic system, Appl. Opt. 22 (2016) 5892.
[10] N.H. Bang, D.X. Khoa, L.V. Doai, Controlling self-Kerr nonlinearity with an external magnetic field in a degenerate two-level inhomogeneously broadened medium, Phys. Lett. A 384 (2020) 126234.
[11] H.M. Dong, N.T. Anh, T.D. Thanh, Controllable Kerr nonlinearity in a degenerate V-type inhomogeneously broadening atomic medium aided by a magnetic field, Opt. Quantum Electron. 54 (4) (2022) 225.
[12] R. Yu, J. Li, P. Huang, A. Zheng, X. Yang, Dynamic control of light propagation and optical switching through an RF-driven cascade-type atomic medium, Phys. Lett. A 373 (2009) 2992.
[13] H.M. Dong, L.V. Doai, V.N. Sau, D.X. Khoa, N.H. Bang, Propagation of laser pulse in a three-level cascade atomic medium under conditions of electromagnetically induced transparency, Photonics Lett. Poland 3 (2016) 73.
[14] D.X. Khoa, H.M. Dong, L.V. Doai, N.H. Bang, Propagation of laser pulse in a three-level cascade inhomogeneously broadened medium under electromagnetically induced transparency conditions, Optik 131 (2017) 497.
[15] H.M. Dong, L.V. Doai, N.H. Bang, Pulse propagation in an atomic medium under spontaneously generated coherence, incoherent pumping, and relative laser phase, Opt. Commun. 426 (2018) 553–557.
[16] G. Huang, K. Jiang, M.G. Payne, L. Deng, Formation and propagation of coupled ultraslow optical soliton pairs in a cold three-state double-Λ-system, Phys. Rev. E 73 (2006) 056606.
[17] Y. Chen, Z. Bai, G. Huang, Ultraslow optical solitons and their storage and retrieval in an ultracold ladder-type atomic system, Phys. Rev. A 89 (2014) 023835.
[18] H.M. Dong, L.T.Y. Nga, D.X. Khoa, N.H. Bang, Controllable ultraslow optical solitons in a degenerated two-level atomic medium under EIT assisted by a magnetic field, Sci. Rep. 10 (1) (2020) 15298.
[19] Zhonghu Zhu, Ai-Xi Chen, Wen-Xing Yang, Ray-Kuang Lee, Phase knob for switching steady-state behaviors from bistability to multistability via spontaneously generated coherence, J. Opt. Soc. Am. B 31 (9) (2014) 2061.
[20] H.R. Hamedi, Optical switching, bistability and pulse propagation in five-level quantum schemes, Laser Phys. 27 (2017) 066002.
[21] H.M. Dong, L.T.Y. Nga, N.H. Bang, Optical switching and bistability in a degenerated two-level atomic medium under an external magnetic field, Appl. Opt. 58 (2019) 4192.
[22] A. Joshi, W. Yang, M. Xiao, Effect of quantum interference on optical bistability in the three-level V-type atomic system, Phys. Rev. A 68 (2003) 015806.
[23] A. Brown, A. Joshi, M. Xiao, Controlled steady-state switching in optical bistability, Appl. Phys. Lett. 83 (2003) 1301.
[24] W. Harshawardhan, G.S. Agarwal, Controlling optical bistability using electromagnetic-field-induced transparency and quantum interferences, Phys. Rev. A 53 (1996) 1812.
[25] S. Gong, S. Du, Z. Xu, Optical bistability via atomic coherence, Phys. Lett. A 226 (1997) 293–297.
[26] D. Cheng, C. Liu, S. Gong, Optical bistability and multistability via the effect of spontaneously generated coherence in a three-level ladder-type atomic system, Phys. Lett. A 332 (2004) 244–249.
[27] D. Zhang, R. Yu, J. Li, C. Ding, X. Yang, Laser-polarization-dependent and magnetically controlled optical bistability in diamond nitrogen-vacancy centers, Phys. Lett. A 377 (2013) 2621.
[28] S.H. Asadpour, A.E. Majd, Controlling the optical bistability and transmission coefficient in a four-level atomic medium, J. Lumin. 132 (2012) 1477–1482.

[29] X. Haifeng, Optical bistability and multistability via both coherent and incoherent fields in a three-level system, Laser Phys. 29 (2019) 015205.
[30] A.H.M. Abdelaziz, A.K. Sarma, Effective control and switching of optical multistability in a three-level V-type atomic system, Phys. Rev. A 102 (2020) 043719.
[31] H. Schmidt, R.J. Ram, All-optical wavelength converter and switch based on electromagnetically induced transparency, Appl. Phys. Lett. 76 (2000) 3173.
[32] B.S. Ham, Nonlinear optics of atoms and electromagnetically induced transparency: dark resonance based optical switching, J. Mod. Opt. 49 (2002) 2477.
[33] S.A. Moiseev, B.S. Ham, Quantum manipulation of two-color stationary light: quantum wavelength conversion, Phys. Rev. A 73 (2006) 033812.
[34] D.D. Yavuz, All-optical femtosecond switch using two-photon absorption, Phys. Rev. A 74 (2006) 053804.
[35] H.M. Dong, N.H. Bang, D.X. Khoa, L.V. Doai, All-optical switching via spontaneously generated coherence, relative phase and incoherent pumping in a V-type three-level system, Opt. Commun. 507 (2022) 127731.
[36] H.M. Dong, N.H. Bang, Controllable optical switching in a closed-loop three-level lambda system, Phys. Scr. 94 (2019) 115510.
[37] M.A. Antón, F. Carreño, O.G. Calderón, S. Melle, I. Gonzalo, Optical switching by controlling the double-dark resonances in a N-tripod five-level atom, Opt. Commun. 281 (2008) 6040.
[38] N.T. Anh, T.D. Thanh, N.H. Bang, H.M. Dong, Microwave assisted all-optical switching in a four-level atomic system, Pramana J. Phys. 95 (2021) 37.
[39] D.X. Khoa, N.V. Ai, H.M. Dong, L.V. Doai, N.H. Bang, All-optical switching in a medium of a four-level vee-cascade atomic medium, Opt. Quantum Electron. 54 (3) (2022) 164.
[40] J. Li, R. Yu, L. Si, X. Yang, Propagation of twin light pulses under magneto-optical switching operations in a four-level inverted-Y atomic medium, J. Phys. B, At. Mol. Opt. Phys. 43 (2010) 065502.
[41] D. Steck, ^{87}Rb D line data, http://steck.us/alkalidata.